Iranian Journal of Oil & Gas Science and Technology, Vol. 5 (2016), No. 2, pp. 45-65
http://ijogst.put.ac.ir

Asphaltene Deposition Modeling during Natural Depletion and Developing a New Method for Multiphase Flash Calculation

Gholamreza Fallahnejad[1] and Riyaz Kharrat[2*]

[1]M.S. Student, Department of Petroleum Engineering, Petroleum University of Technology, Ahwaz, Iran

[2]Professor, Department of Petroleum Engineering, Petroleum University of Technology, Ahwaz, Iran

Received: August 17, 2014; *revised:* January 06, 2015; *accepted:* January 08, 2015

Abstract

The specific objective of this paper is to develop a fully implicit compositional simulator for modeling asphaltene deposition during natural depletion. In this study, a mathematical model for asphaltene deposition modeling is presented followed by the solution approach using the fully implicit scheme. A thermodynamic model for asphaltene precipitation and the numerical methods for performing flash calculation with a solid phase are described. The pure solid model is used to model asphaltene precipitation. The transformation of precipitated solid into flocculated solid is modeled by using a first order chemical reaction. Adsorption, pore throat plugging, and re-entrainment were considered in the deposition model. The simulator has the capability of predicting formation damage including porosity and permeability reduction in each block. A new set of independent unknowns in a fully implicit scheme is presented for asphaltene deposition modeling. In order to find the solution of these variables, the same number of equations is also presented. The description of how to solve the nonlinear system of equations is also described.

Keywords: Asphaltene Deposition, Composition Simulation, Multiphase Flash, Solid Model, Modeling

1. Introduction

Asphaltene precipitation and deposition is a very serious problem that occurs during oil production and processing. Although the problem has been usually observed in the wellbore and the production system, asphaltene precipitation and deposition may occur anywhere in the reservoir-wellbore system including near-wellbore region and inside the wellbore (Darabi et al., 2014).

Various models have been proposed to describe the phase behavior of asphaltene precipitation. According to the literature, there are four main groups for asphaltene precipitation modeling. The first one is the liquid solubility which is based on the Flory-Huggins theory (Flory, 1942). The second models are the solid models which assume that asphaltene is treated as a single component in the solid phase. The third one is the colloidal solution model proposed by Leontaritis and Mansoori (1987) with the consideration of asphaltene as solid particles in a colloidal suspension stabilized by adsorbed resins on asphaltene surface. The fourth one is the thermodynamic micellization model presented by

* Corresponding Author:
Email: kharrat@put.ac.ir

Firoozabadi and Pan (1998). The minimization of the molar Gibbs free energy is the basis of this thermodynamic model.

Few mathematical models were correlated to simulate asphaltene deposition. According to the literature, there are three categories for the asphaltene deposition modeling. The first one is the Leontaritis' model (1998) which assumes that asphaltene deposition occurs only around the wellbore vicinity. The second model is the model of Nghiem et al. (1998) supposing that only adsorption mechanism contributes to the asphaltene deposition. The third one is the model of Wang and Civian (2000) which considers primary physical deposition processes including adsorption, pore throat plugging, and re-entrainment to describe the phenomenon of solid particle deposition.

In this study, the pure solid model is used to model asphaltene precipitation. Also, a deposition model including adsorption, pore throat plugging, and re-entrainment is used. The reduction in the rock porosity and permeability are also included in the asphaltene model. A one-dimensional simulation was carried out for investigating the results of asphaltene deposition model.

2. Mathematical model description

The transportation equations, asphaltene precipitation model, asphaltene deposition model, and the porosity and permeability reduction are considered as the main part of the mathematical model for modeling asphaltene deposition. To develop a simulator for asphaltene deposition, the asphaltene precipitation and deposition models and the porosity and permeability reduction are incorporated into a compositional simulator.

2.1. Asphaltene precipitation model

In this study, a pure solid model is used for predicting the amount of precipitation, while a cubic EOS is applied to the modeling of oil and gas phase behavior. The solid particles are divided into three parts: precipitated, flocculated, and deposited solid. Kohse and Nghiem (2004) proposed a model which assumes that the heaviest component of oil can be split into a non-precipitating and a precipitating component. The precipitated solid is divided into solid 1 which is in equilibrium with the heaviest component in the oil phase and solid 2 that is created from solid 1 via a first order chemical reaction. The fugacity of asphaltene component in the precipitated solid 1 (S_1) is given by:

$$\ln f_{s1} = \ln f_{s1}^{*} + \frac{(Vs(P - P^{*}))}{(RT)} \tag{1}$$

where, f_{s1} is the fugacity of solid S1 at reservoir pressure, and f_{s1}^{*} is the reference solid fugacity at P^{*} ; Vs is the solid molar volume and P^{*} represents the pressure at which the asphaltene just starts to precipitate. Under the thermodynamic equilibrium conditions between S_1, oil, and gas, the following equations must be applied:

$$\ln f_{io} = \ln f_{ig} \quad , i = 1,\ldots,n_c \tag{2}$$

$$\ln f_{n_c,o} = \ln f_{s1} \tag{3}$$

The equality of fugacity of i^{th} component in the oil and gas phases is shown in Equation 2. Equation 3 expresses the equality of fugacity of the precipitating component in the oil phase and in the precipitated solid S_1.

a. Specification of solid molar volume for asphaltene model

For the modeling purpose, solid molar volume is used as a matching parameter. The solid molar volume is initially calculated at reference pressure (P^*) by EOS. Then, we plot the error term versus solid molar volume to find an optimum fit between the calculated and experimental data. The solid molar volume which is used in the plot contains the values around the calculated solid molar volume at the reference pressure. The error term is defined as follows:

$$error = \sum_{i=1}^{n} (W_{(i)\exp} - W_{(i)\mathrm{model}})^2 \tag{4}$$

Figure 1 shows the error term as a function of solid molar volume. The estimated molar volume for the asphaltene component from EOS is $10.5611\ \mathrm{ft}^3/\mathrm{lbmole}$. As can be seen, the minimum error for the given values of solid molar volume is found at $10.81\ \mathrm{ft}^3/\mathrm{lbmole}$.

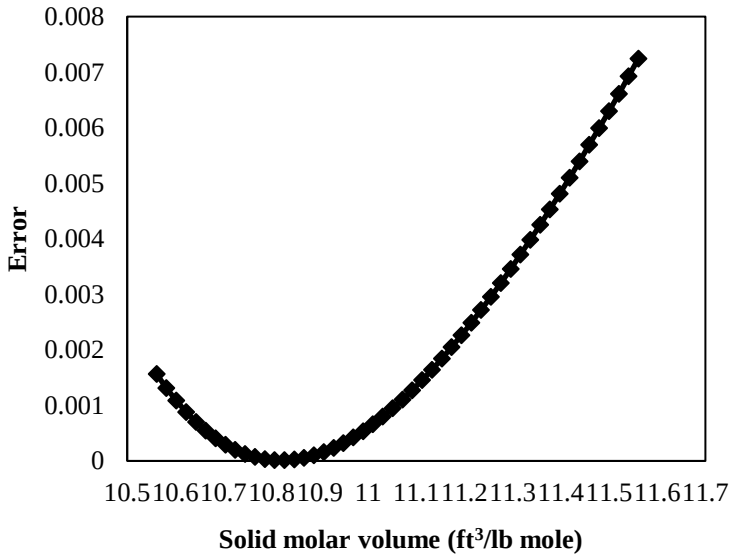

Figure 1
Error term as a function of solid molar volume.

b. Stability test analysis

In multiphase flash calculation, the number of phases is generally unknown beforehand. We use the phase stability analysis to determine the number of phases in each gridblock.

In this study, stability test analysis is separated into two parts: fluid-fluid and fluid-solid stability test.

b.a. Fluid-fluid stability test

The following set of equations (Nghiem and Li, 1984) should be solved to check the stability of a fluid phase (oil) with composition *x*, pressure *P*, and temperature *T*.

$$g_i \equiv lnK_i + ln\varphi_i\left(y,P,T\right) - \ln\varphi_i\left(x,P,T\right) = 0 \tag{5}$$

$$K_i = \frac{Y_i}{x_i} \qquad i = 1,\ldots,n_c \tag{6}$$

where

$$y_i = \frac{Y_i}{\sum_{j=1}^{n_c} Y_j} \tag{7}$$

If Equation 5 is solved for Y_i at a given P and T, a solution is found that

$$\sum_{j=1}^{n_c} Y_j > 1 \tag{8}$$

The mixture x is unstable at P and T.

Equation 5 can be solved with the QNSS method (Nghiem and Li, 1984). With the QNSS, let α be the vector with elements lnK_i, and let α^k be the k^{ih} iteration value for the vector α. The QNSS iteration is given by:

$$\overline{\Delta\alpha}^{(k)} = \bar{\alpha}^{k+1} - \bar{\alpha}^{k} \tag{9}$$

$$\overline{\Delta\alpha}^{(k)} = -\xi^{(k)}\bar{g}^{(k)} \tag{10}$$

And ξ is a scalar given by:

$$\xi^{(k)} = \xi^{(k-1)}\left(\frac{\overline{\Delta\alpha}^{(k-1)}.\bar{g}^{(k-1)}}{\overline{\Delta\alpha}^{(k-1)}.\overline{\Delta g}^{(k-1)}}\right) \tag{11}$$

where

$$\bar{g} = norm\left(g\right) \tag{12}$$

$$\bar{\alpha} = norm\left(\alpha\right) \tag{13}$$

The process is initialized with $\xi^{(0)} = 1$ and α is started with Wilson equation.

Figure 2 shows a flow chart for this procedure.

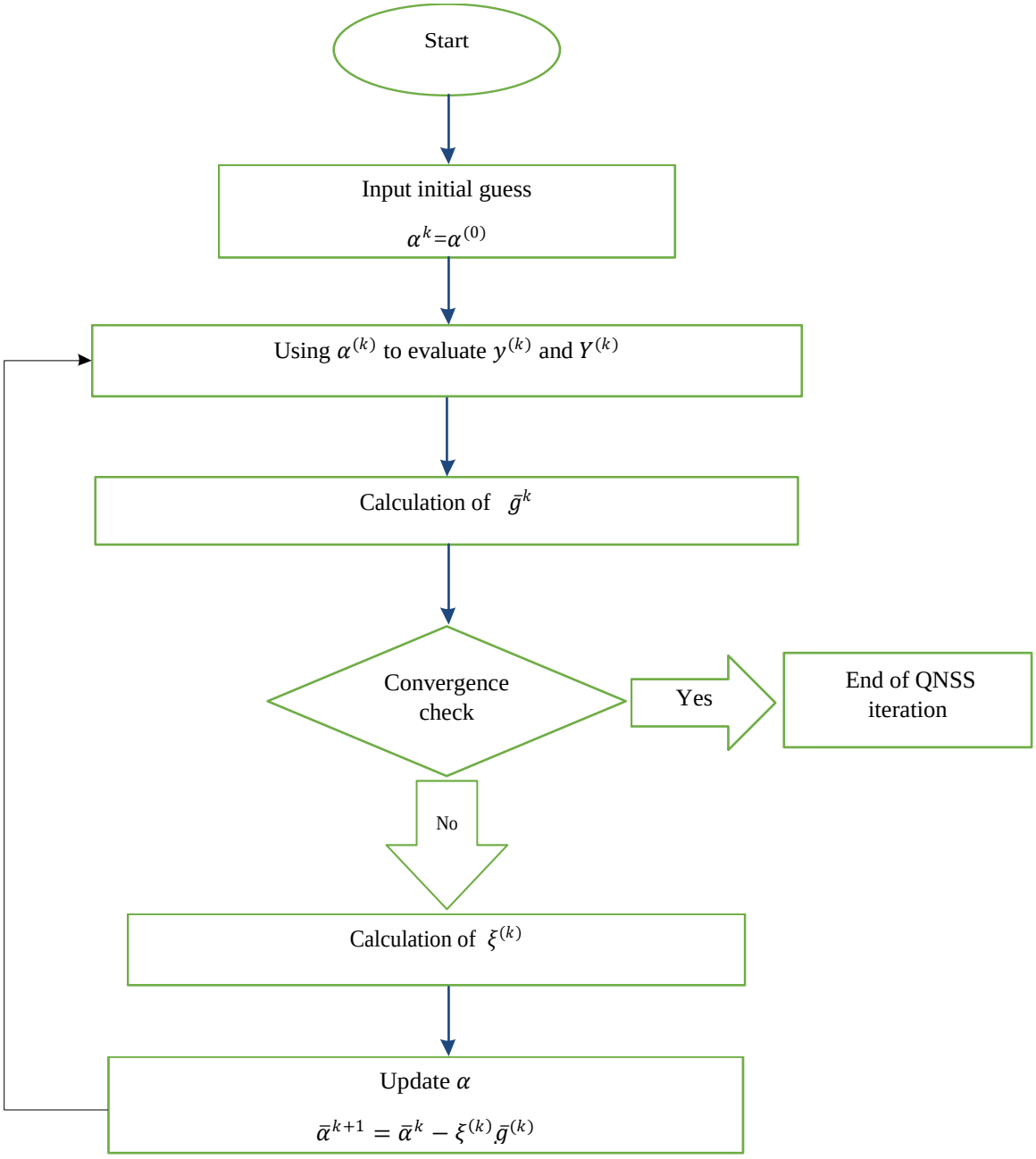

Figure 2
QNSS iteration for fluid-fluid stability test.

b. Fluid-solid stability test

To test the existence of solid phase, the following criteria should be satisfied. The solid phase exists if:

$$\ln f_{n_c o} \geq ln\, f_{s1} \tag{14}$$

This implies that if the fugacity of the asphaltene component in the solid phase is less than the fugacity of the n_c^{th} component in the oil phase, more asphaltene precipitation will occur until both fugacities become equal. Figure 3 depicts the stability test calculation procedure.

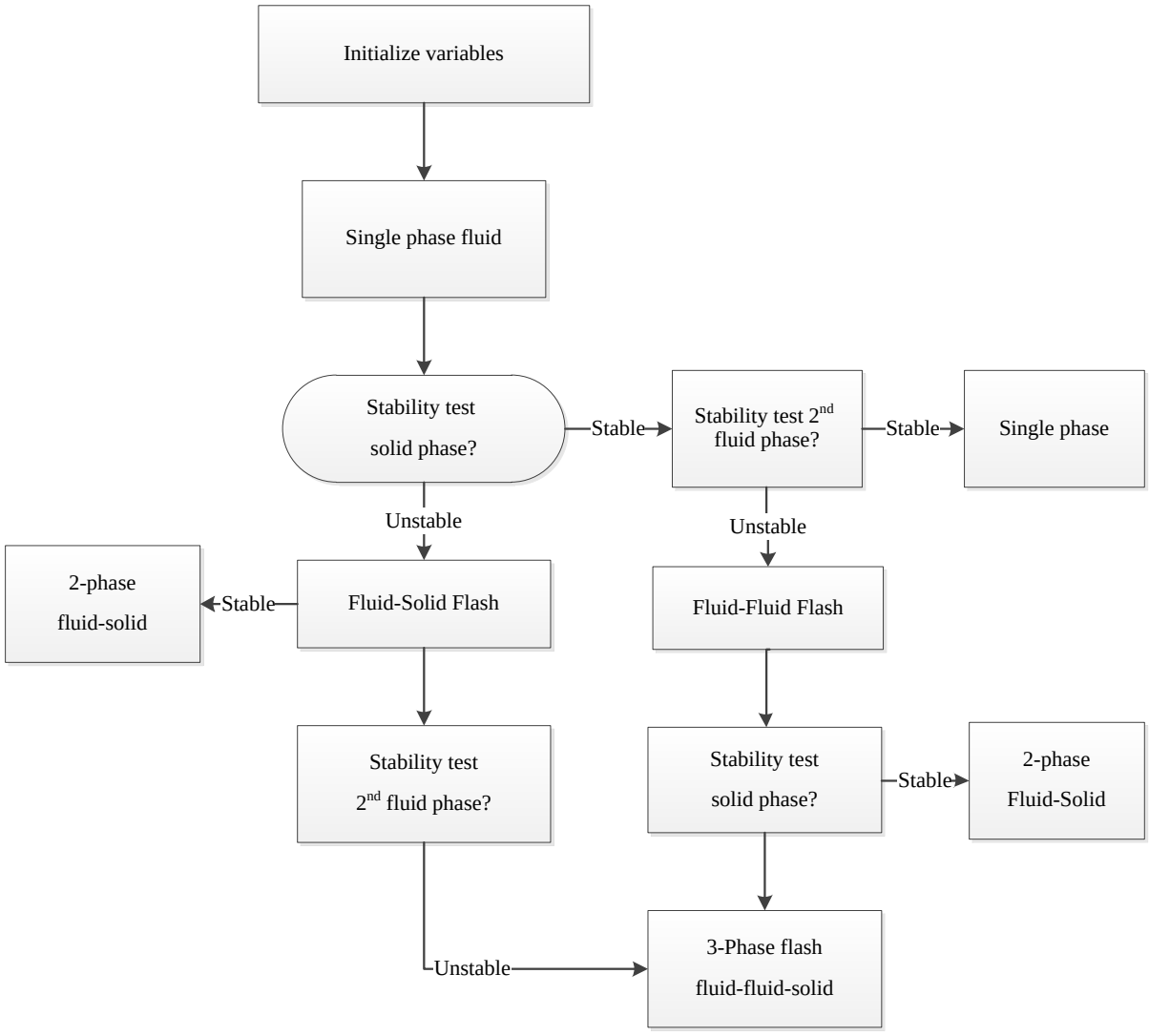

Figure 3
Stability test analysis.

c. Multiphase flash calculations

The set of independent variables involved for the flash calculation are $Ln(K_i), Ks, Lg$, and Ls, which gives n_c+3 unknowns. The following set of equations should be used for solving these variables:

$$\ln K_{ig} + \ln \varphi_{ig} - \ln \varphi_{io} = 0 \tag{15}$$

$$\ln K_{n_c s} + \ln \varphi_s - \ln \varphi_{n_c o} = 0 \tag{16}$$

With

$$K_{ig} = \frac{y_{ig}}{y_{io}} \tag{17}$$

$$\varphi_{ij} = \frac{f_{ij}}{y_{ij} P} \qquad j=o \text{ and } g \tag{18}$$

$$K_{n_c s} = \frac{1}{y_{nco}} \tag{19}$$

$$\varphi_s = \frac{f_s}{P} \tag{20}$$

In conjunction with the above equations, the following material balance equations can be derived:

$$\sum_{i=1}^{nc} \frac{\left(K_{ig} - 1\right) z_i}{1 + L_g \left(K_{ig} - 1\right) + L_s \left(K_{is} - 1\right)} = 0 \tag{21}$$

$$\sum_{i=1}^{nc} \frac{\left(K_{is} - 1\right) z_i}{1 + L_g \left(K_{ig} - 1\right) + L_s \left(K_{is} - 1\right)} = 0 \tag{22}$$

The oil and gas phase composition can be calculated from the following equations:

$$y_{io} = \frac{z_i}{1 + L_g \left(K_{ig} - 1\right) + L_s \left(K_{is} - 1\right)} \tag{23}$$

$$y_{ig} = K_{ig} x_{io} \tag{24}$$

There are n_c+3 nonlinear equations and unknowns for multiphase flash calculations. The unknown vector is considered as follows:

$$\vec{X}_i = \left(Ln(K_{ig}), K_s, L_g, L_s\right) \tag{25}$$

To solve the nonlinear system of equations, the Newton method is used, where the residual vector ($\vec{\mathbf{R}}$) is computed. The residual vector consists of Equations 15, 16, 21, and 22.

The detailed multiphase flash calculation procedure is given in Figure 4.

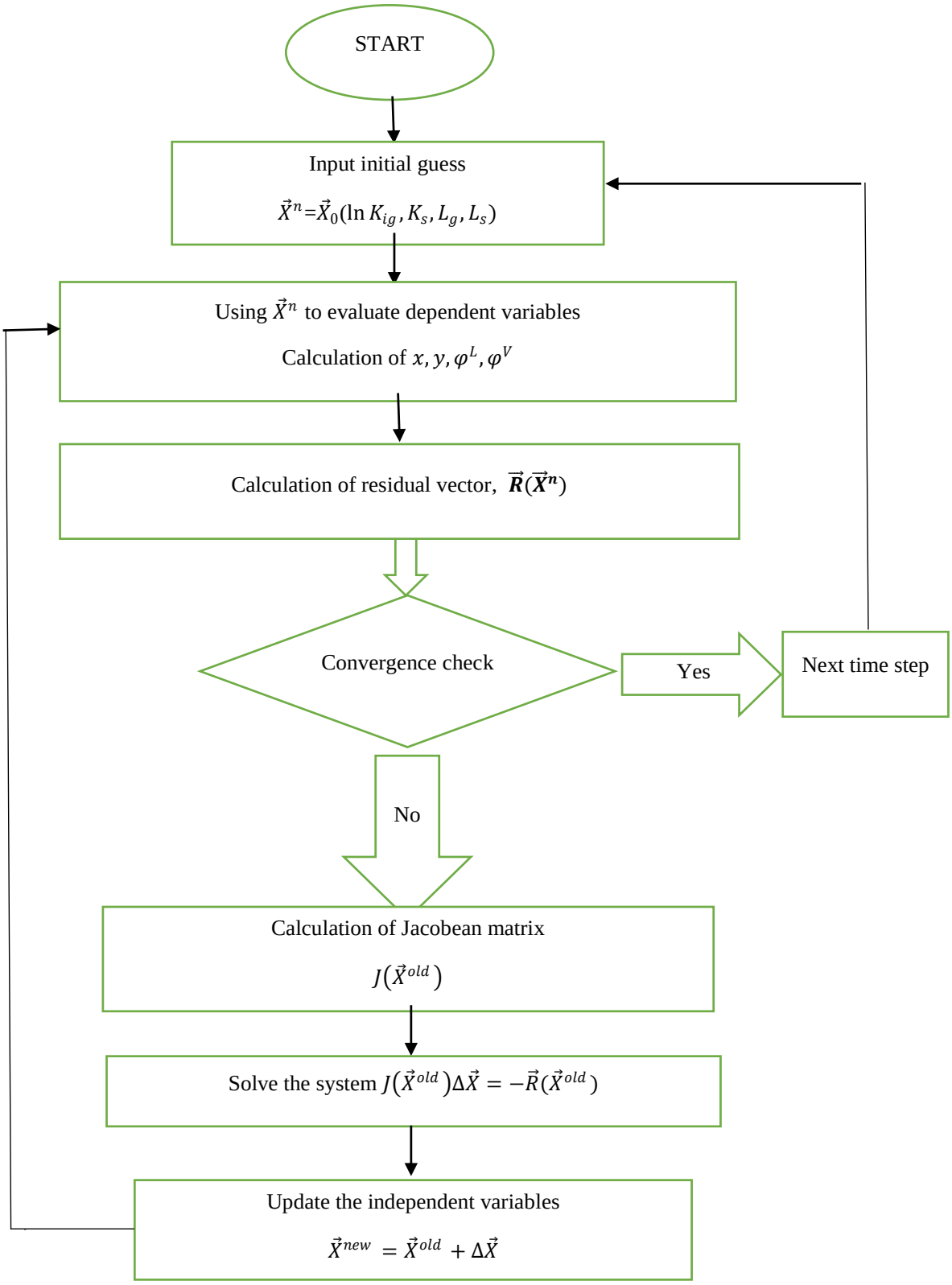

Figure 4
Flow chart for flash calculations procedure.

2.2. Asphaltene deposition model

In this study, the model of Wang and Civian (2000) is used to simulate the formation damage caused by asphaltene deposition during natural depletion. This model has three terms, including adsorption, pore throat plugging, and re-entrainment to describe asphaltene deposition process. The deposition equation is presented as follows:

$$\frac{\partial E_A}{\partial t} = \alpha \phi C_A - \beta E_A (v_L - v_{cr,L}) + \gamma u_L C_A \tag{26}$$

2.3. Porosity and permeability reduction model

Once asphaltene deposition occurs, porosity alteration is modeled by the following equation:

$$\phi = \phi_0 - E_A \tag{27}$$

To update the permeability values, a power law relationship is used as given below:

$$R_f = \frac{K_0}{K} = \left(\frac{\phi_0}{\phi} \right)^3 \tag{28}$$

2.4. Compositional simulator equations

Compositional simulator includes component molar flow equations, phase equilibrium equations, multiphase flash equations, and saturation constraint equations, which are solved simultaneously.

a. Component molar balance equations

The following material balance equation with the consideration of asphaltene can be written:

$$\nabla\left(\xi_o y_{jo} \nabla\Phi_o\right) + \nabla\left(\xi_g y_{jg} \nabla\Phi_g\right) + q_j = \frac{\partial\left(\phi N_j\right)}{\partial t} \quad j = 1,\ldots,n_c - 1 \tag{29}$$

$$\nabla\left(\xi_o (y_{n_c o} + y_{s_1} + y_{s_2}) \nabla\Phi_o\right) + \nabla\left(\xi_g y_{n_c g} \nabla\Phi_g\right) + q_{n_c} = \frac{\partial\left(\phi N_{n_c}\right)}{\partial t} \tag{30}$$

where,

N_i is the moles of component *i* per pore volume (lbmole/ft^3);

y_{ik} is the mole fraction of component *i* in phase *k* (*k* = o,g);

y_{sj} is the mole fraction of suspended solid in oil phase (*j* = 1, 2);

ξ_k is the molar density of phase *k* (*k* = o,g) (lbmole/ft^3);

A material balance on solid S_2 completes transport equations:

$$\nabla\left(\xi_o y_{s_2} \nabla\Phi_o\right) + V_b \phi S_o r + q_{s_2} = \frac{\partial\left(\phi N_{s_2}\right)}{\partial t} \tag{31}$$

$$y_{s1} = \frac{N_T^{'} L_s}{N_o} \tag{32}$$

$$y_{s2} = \frac{N_{s2}}{N_o} \tag{33}$$

$$r = K_{12} C_{s1,o} - K_{21} C_{s2,o} \tag{34}$$

where,

$$C_{s1,o} = \frac{N_T^{'} L_s}{S_o} \tag{35}$$

$$C_{s1,o} = \frac{N_{s2}}{S_o} \tag{36}$$

b. Phase equilibrium equations

The following equations for thermodynamic equilibrium between S_1, oil, and gas must be applied:

$$\ln f_{io} = \ln f_{ig} \ , i = 1,\ldots,n_c \tag{37}$$

$$\ln f_{n_c,o} = \ln f_{s1} \tag{38}$$

c. Phase composition constrains

The following equations are used to consider the phase composition constrains:

$$\sum_{i=1}^{n_c} y_{io} - \sum_{i=1}^{n_c} y_{ig} = 0 \tag{39}$$

$$\sum_{i=1}^{n_c} y_{io} - \sum_{i=1}^{n_c} y_{is} = 0 \tag{40}$$

d. Volume constraint equation

The volume constraint equation expresses that the pore volume in each grid must be occupied by the total fluid volume. This equation can be written as follows:

$$\sum_{j=1}^{n_p} S_j - 1 = 0 \tag{41}$$

3. Solution approach

After finite differencing, there are $(2n_c + 6)n_b$ nonlinear equations for n_b number of gridblocks. Equations 28, 29, 30, 36, 37, 38, 39, 40, and 25 provide a system of nonlinear equations that can be solved for $(Ni, Ln(Ki), Ns_2, Ns_3, P, Ks, Lg, Ls)$ for each gridblock. A fully implicit technique is used

to solve the governing equation for these independent variables. The unknown vector is considered as follows:

$$\vec{\mathbf{X}}_{\mathbf{i}} = \left(N_i, Ln(Ki), Ns_2, Ns_3, P, Ks, Lg, Ls\right) \tag{42}$$

A Newton method is used to linearize the governing equations in terms of the independent variables. The solution procedure is described as follows:

Input initial

1. The solution vector at the old time step is usually set as the initial guess for the new time step;
2. Using initial guess vector to compute dependent variables such as porosity, molar density, relative permeability, molar composition, phase viscosities, and source or sink;
3. Calculate the residual vector and check for the convergence. If convergence is achieved, the guessed solution vector is considered as the true solution for the new time step. If a tolerance is exceeded, another solution vector is guessed and the independent variables are updated. The new solution vector is obtained by solving the system $J(\vec{X}^{old})\Delta\vec{X} = -\vec{R}(\vec{X}^{old})$ where the Jacobian matrix (J) and the residual vector are computed using the previous solution vector. Independent variables are updated as follows:

$$\vec{\mathrm{X}}^{\mathrm{new}} = \vec{\mathrm{X}}^{\mathrm{old}} + \Delta\vec{\mathrm{X}} \tag{43}$$

4. Results and discussion

In this section, the results of the implemented asphaltene model which is obtained from a 1D simulation case are presented. Table 1 shows the composition of oil used for studying asphaltene precipitation, which is obtained from the work of Burke et al. (1990). The reservoir properties are given in Table 2.

Table 1
Modeled fluid composition.

Component	mole %	MW
CO_2	2.46	44.010
N_2	0.57	28.013
C_1	36.37	16.043
C_2	3.47	30.070
C_3	4.05	44.097
i-C_4	0.59	58.124
n-C_4	1.34	58.124
i-C_5	0.74	72.151
n-C_5	0.83	72.151
FC_6	1.62	86.000
C_7-C_{15}	19.66	147.272
C_{16}-C_{25}	12.55	279.2
C_{26}-C_{30}	4.00	389.52
C31A+	7.42	665.624
C31B+	4.32	665.624

Table 2
Simulation input data.

Parameter	Value
No. of gridblocks	21
Reservoir size	500×10×10 ft3
Reservoir Temperature	212 °F
Initial water saturation	0
Initial reservoir pressure	6014.7 psi
Porosity	0.2
Permeability	30 md
Production constraint	2.5 bbl./day
Rock compressibility	5×10^{-6} psi-1
Ref. P for rock compressibility	14.7 psi

The reservoir is one-dimensional homogenous with the size of $500\times 10 \times 10$ ft^3 and divided into 21 gridblocks. The porosity and permeability are 0.2 and 30 mD respectively. The initial reservoir pressure is 6014.7 psia and reservoir temperature is 212 °F. The well is located at the center of the reservoir at the constant bottomhole reservoir fluid rate (BHF) of 2.5 bbl./day. The input parameters for the precipitation, deposition, and flocculation models, which are taken from Kohse and Nghiem (2004), are shown in Table 3. In this study, it is assumed that the interstitial velocity is less than the critical interstitial velocity; as a result, the entrainment rate coefficient β is set to zero. The liquid-gas relative permeability curves and the liquid-gas capillary pressure curve for the simulation case are shown in Figures 5 and 6.

Table 3
Asphaltene precipitation, deposition, and flocculation model parameters.

Parameter	Value
P^*	4014.7 psi
$ln f_{n_{cs}}^*$	-25.223 psi
V_s	10.812 lbm/ft^3
k 12 (day^{-1})	0.1
k 21 (day^{-1})	0.08
α (day^{-1})	0.01
β (ft^{-1})	0.0
γ (ft^{-1})	0.05
σ	150

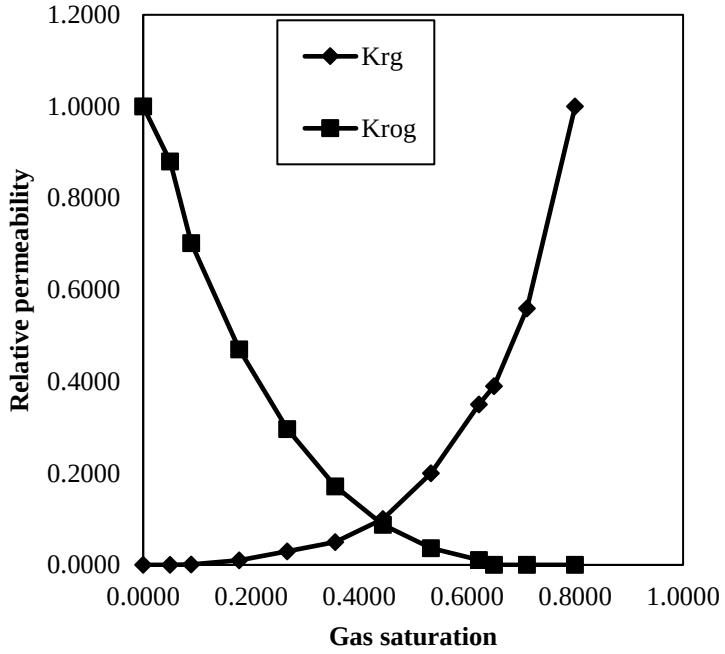

Figure 5
The liquid-gas relative permeability curves.

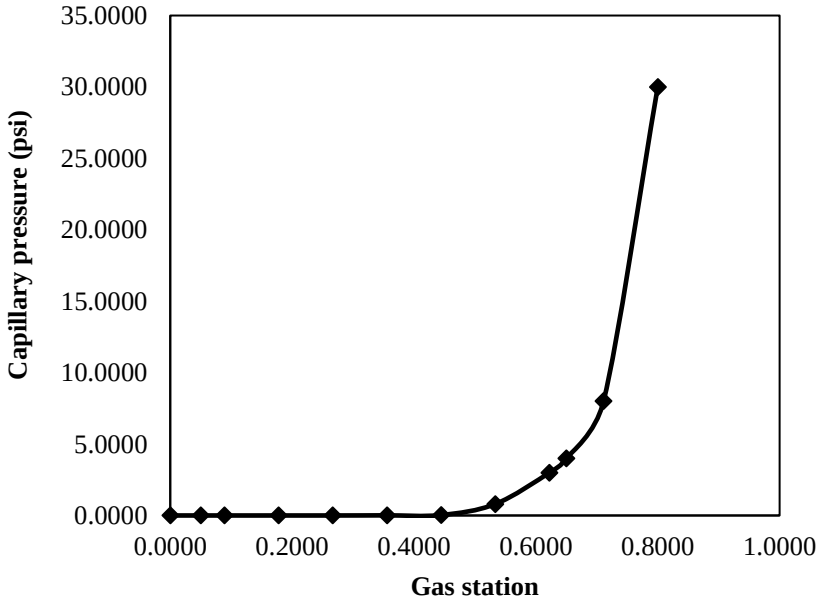

Figure 6
The liquid-gas capillary pressure curve.

Figure 7 presents pressure versus time for the gridblock (11,1,1). As can be seen, the initial reservoir pressure, the onset pressure (P^*) of asphaltene, and saturation pressure are 6014.7, 4550, and 2950 psia respectively. The onset pressure for asphaltene precipitation will be reached after approximately 13 days of production time. The saturation pressure will be reached after 30 days of production time. The pressure depletion continues to reach a value of 2223.4 at the end of simulation time.

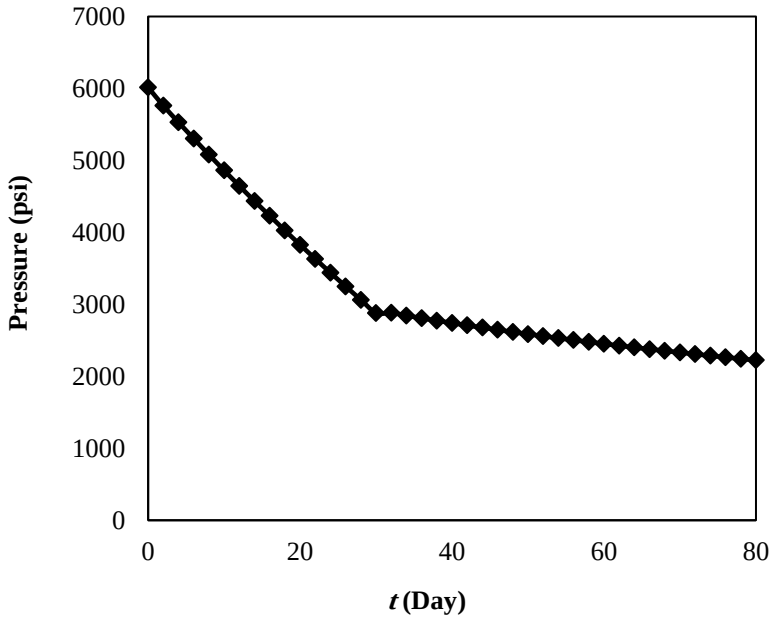

Figure 7
Pressure profile at gridblock (11,1,1) after 80 days.

Oil and gas saturation are depicted in Figure 8. As can be seen, the oil saturation remains constant until the bubble point pressure is reached. After 30 days of production time the oil saturation gradually decreases and will be reached the value of 0.9 at the end of simulation time.

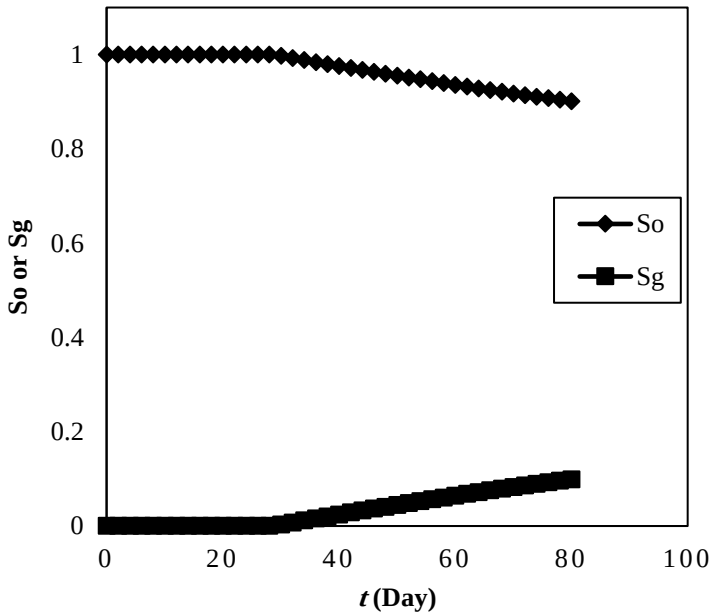

Figure 8
Oil and gas saturation at gridblock (11, 1, 1).

Porosity versus time is presented in Figure 9. As this figure shows, the porosity reduction shows a sharper trend after saturation pressure is reached. Both pressure depletion and asphaltene deposition are the causes for porosity alteration.

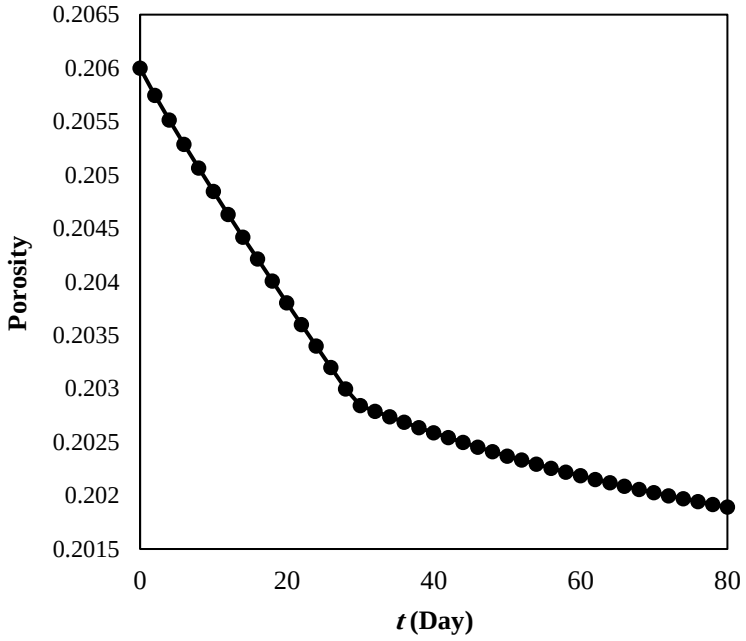

Figure 9
Porosity at gridblock (11, 1, 1).

Permeability reduction (K/K_i) is reported in Figures 10. This parameter has an important role in asphaltene precipitation studies. A uniform decline of permeability can be seen in this plot.

Figure 11 shows how the productivity index varies with time. This parameter also shows the same trend as permeability reduction. As can be seen, after 30 days of production time, in addition to asphaltene deposition, oil relative permeability reduction plays an important role in the productivity index reduction; as a result, this parameter starts decreasing sharply after 30 days.

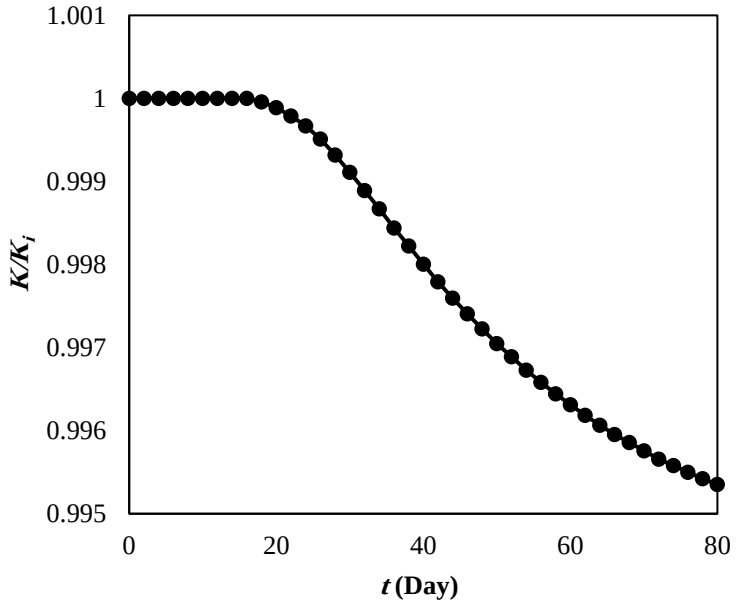

Figure 10
Ratio of the damage permeability to the original permeability.

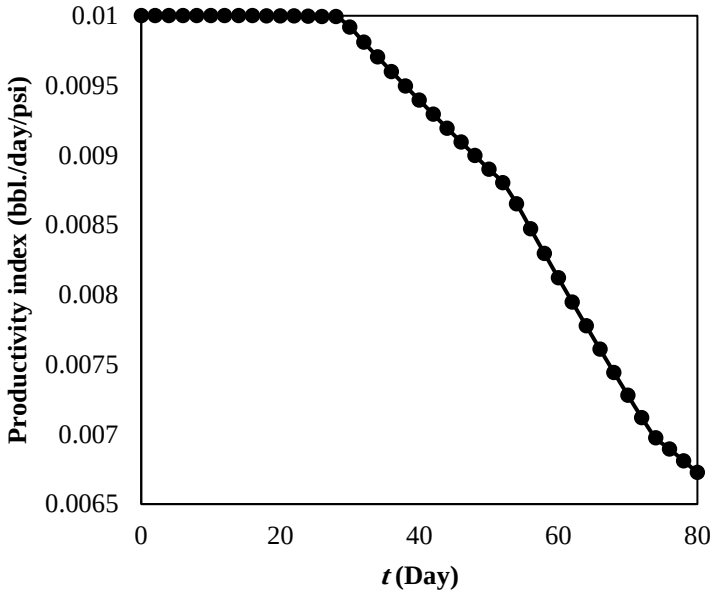

Figure 11
Productivity index versus time at well-block.

Figure 12 illustrates the amount of precipitated asphaltene (mole per pore volume lbmole/ft^3) versus time during the simulation time. As can be seen, after 12 days of simulation time, the precipitation is started. The maximum value of precipitation occurs around the saturation pressure and decreases as pressure drops further.

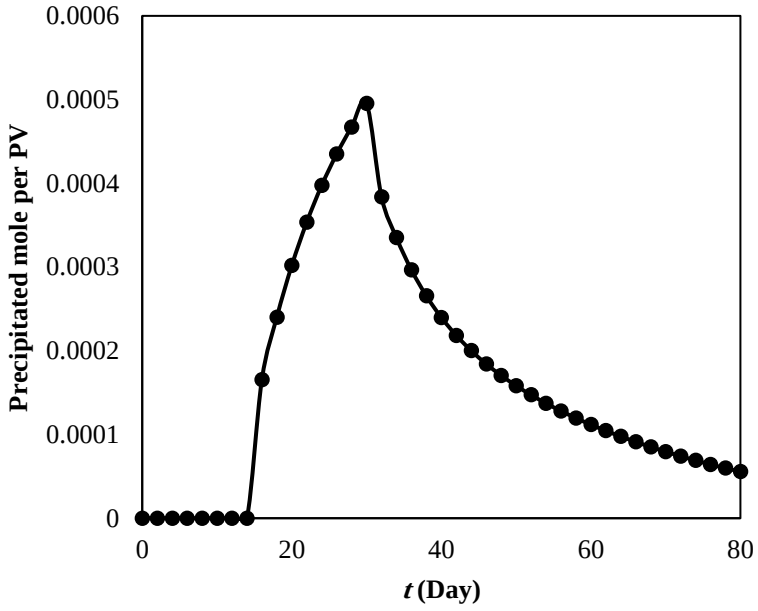

Figure 12
Asphaltene precipitated mole per pore volume at gridblock (11,1,1).

Figure 13 shows the amount of flocculated asphaltene (mole per pore volume lbmole/ft^3) versus time during the simulation time. As can be seen, the trend of plot is the same as the plot of asphaltene

precipitation, but there is a time interval between the maximum value of the precipitation and flocculation.

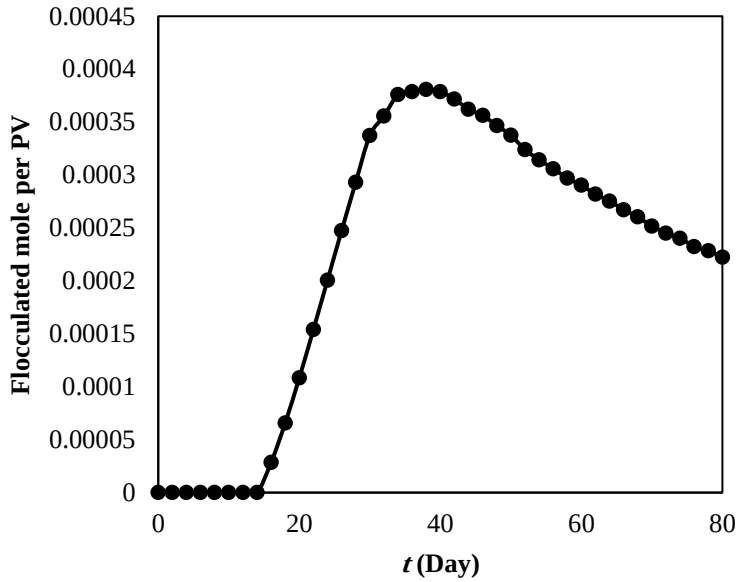

Figure 13
Asphaltene flocculated mole per pore volume at gridblock (11,1,1).

The amount of deposited asphaltene (mole per pore volume lbmole/ ft^3) with respect to production time is shown in Figure 14. The gradual increase of deposited asphaltene at gridblock (11,1,1) is shown in this figure.

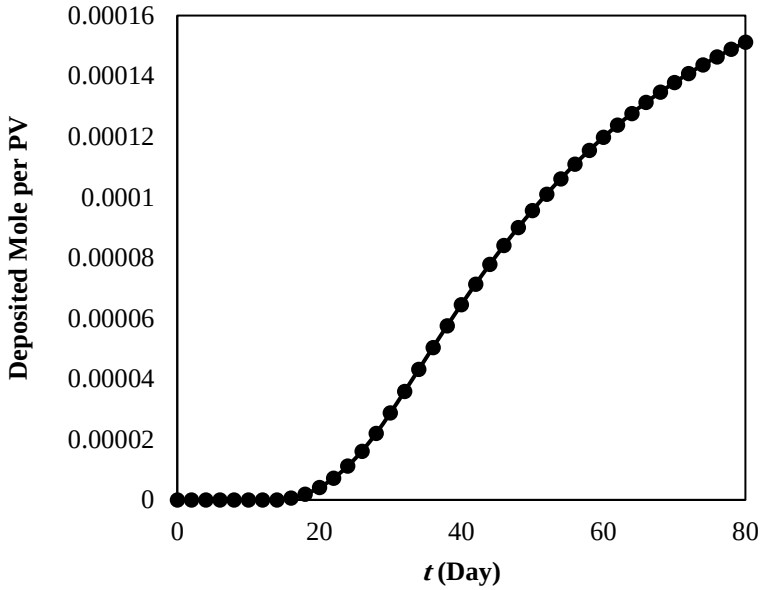

Figure 14
Asphaltene deposited mole per pore volume at gridblock (11,1,1).

Figures 15 and 16 show the comparison of the precipitated and deposited asphaltene profile between Matlab code and CMG GEM during 80 days of simulation time respectively. As can be seen, because

of considering new multiphase flash calculation approach, the deposited asphaltene profile gives a better match than the precipitated profile. As a matter of fact, in the deposited profile, in addition to thermodynamic equations, material balance equations play a great role, and since it regards the new approach to multiphase flash calculation, the material balance equations would change. As a result, a clear difference between Matlab code and CMG GEM can be seen for the deposited asphaltene profile compared to the precipitated profile.

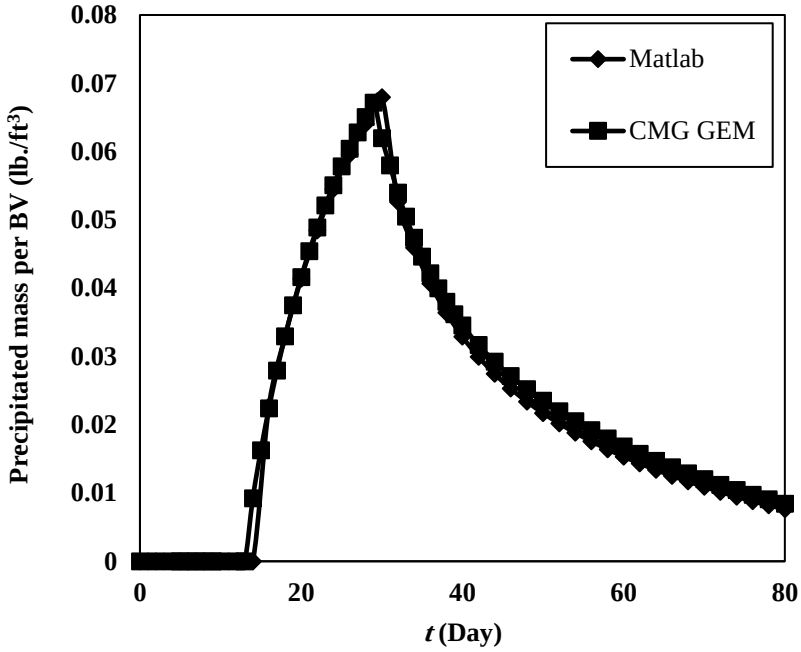

Figure 15
Asphaltene precipitated mass per bulk volume at gridblock (11,1,1).

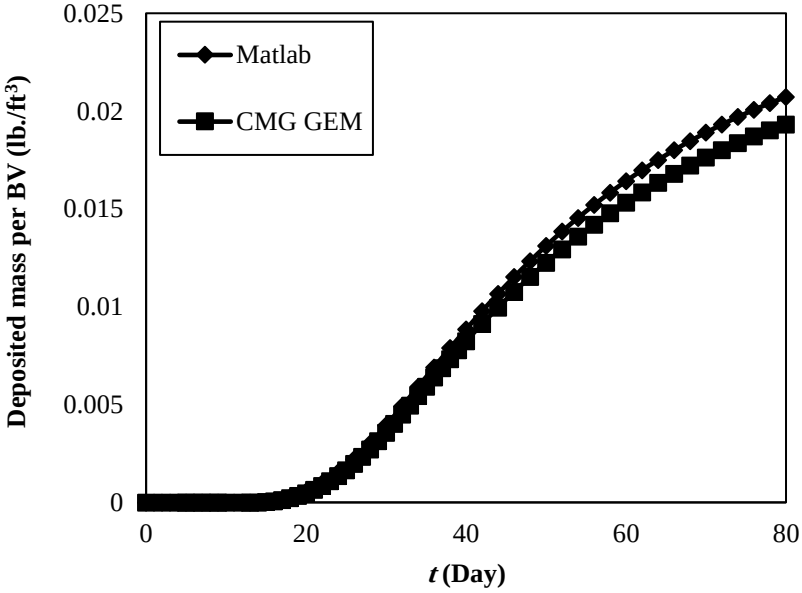

Figure 16
Asphaltene deposited mass per bulk volume at gridblock (11,1,1).

5. Conclusions

This paper presents the modeling of the phase behavior and dynamic aspects of asphaltene precipitation and deposition for natural depletion. A solid model is used to model asphaltene phase behavior. The thermodynamic model for asphaltene precipitation has been successfully incorporated into a fully implicit compositional simulator, where the phase equilibrium equations, the saturation constraint equation, the component transport equations, the multiphase flash equations, and the deposition equation are solved simultaneously for each gridblock. Just a part of the precipitated asphaltene is considered to adsorb to the rock and the remaining part is considered to stay suspended in the oil phase. A resistance factor model was introduced for the estimation of the effect of asphaltene precipitation on relative permeability.

Nomenclature

$C_{s_1 o}$: Concentration of suspended solid s_1 in oil phase [lbmole/ft^3]

$C_{s_2 o}$: Concentration of suspended solid s_2 in oil phase [lbmole/ft^3]

$C_{s_2^f}$: Volumetric concentration of flowing solid s_2 per volume of oil [-]

f_{ig} : Fugacity of component *i* in gas phase [psi]

f_{io} : Fugacity of component *i* in oil phase [psi]

f_{s1}^* : Reference solid fugacity [psi]

f_{s1} : Fugacity of solid s_1 [psi]

n_b : Total number of gridcells

n_c : Number of hydrocarbon components

N_i : Moles of component *i* per pore volume [lbmole/ft^3]

N_{s1} : Moles of solid s_1 per pore volume [lbmole/ft^3]

N_{s2} : Moles of solid s_2 per pore volume [lbmole/ft^3]

N_{s3} : Moles of deposited solid per pore volume [lbmole/ft^3]

N_T : Total number of moles per pore volume [lbmole/ft^3]

N_T' : Total number of moles without flocculated and deposited solid per pore volume [lbmole/ft^3]

u_o : Oil phase Darcy velocity [ft/day]

V : Gridblock volume [ft^3]

$V_{cr,o}$: Critical oil phase interstitial velocity [ft./day]

$V_{s_2^d}$: Volume of deposited solid s_2 per gridblock volume [-]

y_{ik} : Mole fraction of component *i* in phase *k* (*k* = o,g) [-]

y_{sj} : Mole fraction of suspended solid in oil phase (*j* = 1, 2) [-]

z_i : Global mole fraction of component *i* in feed [-]

Greeks

α : Surface deposition rate coefficient [day^{-1}]

β : Entrainment rate coefficient [ft^{-1}]

γ : Pore throat plugging rate coefficient [ft^{-1}]

φ_{ij} : Fugacity coefficient of component *i* in phase *j*

ξ_k : Molar density of phase *k* (*k* = o,g) [lbmole/ft^3]

v_o : Oil phase interstitial velocity [ft./day]

v_s : Solid molar volume [ft^3/lbmole]

Subscripts

g : Gas

o : Oil

References

Ali, M. A. and Islam, M. R., The Effect of Asphaltene Precipitation on Carbonate Rock Permeability: an Experimental and Numerical Approach, Paper SPE 38856 presented at the SPE Annual Technical Conference and Exhibition, San Antonio, 5–8 October, 1997.

Burke, N. E., Hobbs, R. D., and Kashou, S. F., Measurement and Modeling of Asphaltene Precipitation, JPT, Vol. 42, No. 11, p. 1440-1446, 1990.

Choiri, M., Study of CO_2 Effect on Asphaltene Precipitation and Compositional Simulation of Asphaltenic Oil Reservoir, M.Sc. Thesis, The University of Stavanger, 2010.

Computer Modeling Group, Win Prop and GEM Manual, 2007.

Darabi, H., Shirdel, M., Kalaei, M. H., and Sepehrnoori, K., Aspects of Modeling Asphaltene Deposition in a Compositional Coupled Wellbore/ Reservoir Simulator, SPE 169121, Presented at SPE Annual Technical Conference and Exhibition, Tulsa, Oklahoma, USA, 12–16 April 2014.

ECLIPSE Technical Description, The Asphaltene Option, p. 89 – 102, 2010.

Fazelipour, W., Development of a Fully Implicit, Parallel, EOS Compositional Simulator to Model Asphaltene Precipitation in Petroleum Reservoirs, M.Sc. Thesis, The University of Texas at Austin, 2007.

Fazelipour, W., Pope, G., and Sepehrnoori, K., Development of a Fully Implicit, Parallel, EOS Compositional Simulator to Model Asphaltene Precipitation in Petroleum Reservoirs, SPE 120203, Presented at SPE Annual Technical Conference and Exhibition, 2008.

Hirschberg, A., Dejong, L. N. J., Schipper, B. A. and Meijer, J. G., Influence of Temperature and Pressure on Asphaltene Flocculation, Paper SPE 11202, June, 1984

Kohse B., Nghiem L. X., Modeling Asphaltene Precipitation and Deposition in a Compositional Reservoir Simulator, SPE No. 89437, 14 the Symposium Improved Oil Recovery, Tulsa, Oklahoma, April 2004.

Leontaritis, K. J. and Mansoori, G. A., Asphaltene Flocculation during Oil Production and Processing: A Thermodynamic-colloidal Model, Paper SPE 16258 presented at the SPE International Symposium on Oil Field Chemistry, San Antonio, January1987.

Leontaritis, K. J. and Mansoori, G. A., Asphaltene Deposition: A Survey of Field Experiences and Research Approaches, Journal of Petroleum Science and Engineering, Vol. 1, N0. 3, p. 229–239, 1988.

Leontaritis, K., Asphaltene Near-wellbore Formation Damage Modeling, SPE 39446, Presented at SPE Formation Damage Control Conference, Lafayette, Louisiana, 18-19 February, 1998.

Leontaritis, K. J. and Mansoori, G. A., Asphaltene Deposition, a Survey of Field Experiences and Research Approaches, Journal of Petroleum Science and Engineering, Vol. 1, No. 3, p. 229-239, 1988.

Nghiem, L. X., Hassam M. S. and Nutakki R., Efficient Modeling of Asphaltene Precipitation, Presented at the 1993 SPE Annual Technical Conference and Exhibition, Paper SPE 26642, Houston, TX, Oct 3-6, 1993.

Nghiem L.X., Coombe D.A., Modeling of Asphaltene Precipitation during Primary Depletion, Paper No. SPE 36106, Fourth Latin American and Caribbean Petroleum Engineering Conference, Port of Spain, Trinidad and Tobago, 23-26 April 1996.

Nghiem, L.X., and Dennis, A., Modeling Asphaltene Precipitation during Primary Depletion, Paper SPE 36106 Presented at IV Latin American/Caribbean Petroleum Engineering Conference, Trinidad and Tobago, 23–26 April, 1996.

Nghiem, L. X., Phase Behavior Modeling and Compositional Simulation of Asphaltene Deposition in Reservoirs, Ph.D. Thesis, University of Alberta, Department of Civil and Environmental Engineering, 1999.

Nghiem, L. X., Kohse, B. F., Farouq-Ali, S. M., and Doan, Q., Asphaltene Precipitation: Phase Behavior Modeling and Compositional Simulation, Paper SPE 59432 Presented at the SPE Asia Pacific Conference on Integrated Modeling for Asset Management, Yokohama, 25–26 April, 2000.

Pan, H. and Firoozabadi, A., Thermodynamic Micellization Model for Asphaltene Aggregation and Precipitation in Petroleum Fluids, SPE Production & Facilities, Vol. 13, No.2, p.118–127, May 1998.

Shirdel, M., Development of a Coupled Wellbore-reservoir Compositional Simulator for Damage Prediction and Remediation, Ph.D. Dissertation, The University of Texas at Austin, 2013.

Wang, S., Simulation of Asphaltene Deposition in Petroleum Reservoirs During Primary Oil Recovery, Ph.D. Dissertation, The University of Oklahoma, December, 2000.

Wang, S., Civan, F., and Strycker, A. R., Simulation of Paraffin and Asphaltene Deposition in Porous Media SPE Paper No, 50746 Presented at the SPE 1999 International Symposium on Oilfield Chemistry, Houston, Texas, February 16-19,1999.